AJNR

Preliminary Experience Using Contrast-Enhanced MR Angiography to Assess Vertebral Artery Structure for the Follow-up of Suspected Dissection

Xavier Leclerc, Christian Lucas, Olivier Godefroy, Lionel Nicol, Aline Moretti, Didier Leys and Jean Pierre Pruvo

AJNR Am J Neuroradiol 1999, 20 (8) 1482-1490
http://www.ajnr.org/content/20/8/1482

AJNR Am J Neuroradiol 20:1482–1490, September 1999

Preliminary Experience Using Contrast-Enhanced MR Angiography to Assess Vertebral Artery Structure for the Follow-up of Suspected Dissection

Xavier Leclerc, Christian Lucas, Olivier Godefroy, Lionel Nicol, Aline Moretti, Didier Leys, and Jean Pierre Pruvo

BACKGROUND AND PURPOSE: **Important advances have been made recently in MR angiography with the use of contrast medium injection, which has proved valuable for the imaging of vertebral arteries (VAs) obtained during short scanning times. Our purpose was to assess the feasability of contrast-enhanced fast 3D MR angiography for imaging VAs and to evaluate the long-term follow-up of VA dissections.**

METHODS: **Sixteen consecutive patients with 18 angiographically documented VA dissections (seven occlusive dissections and 11 stenotic dissections, including two each with a pseudoaneurysm) were followed up using both contrast-enhanced 3D MR angiography and cervical T1-weighted MR imaging at a median delay of 22 months. Ten patients underwent MR imaging at the acute phase as well, and nine underwent early follow-up angiography at a median delay of 3 months. MR angiographic findings were determined by consensus, focussing on image quality, presence of residual stenosis, luminal irregularities, and occlusion.**

RESULTS: **Of the 32 VAs, a segment of the artery was not assessable on contrast-enhanced MR angiography in each of four small VAs. A central signal void artifact of cervical arteries was seen in one patient and motion artifacts were seen in two, but images could be interpreted. A venous enhancement was detected in 10 of 16 examinations, but this did not prevent image analysis. Ten of 11 stenotic dissections returned to normal, whereas one stenotic dissection progressed to occlusion. Two pseudoaneurysms detected by initial angiography resolved spontaneously; one was revealed only by delayed MR angiography, and one was detected on an early MR angiogram and proved resolved on a late MR angiogram. Of the seven initially occluded VAs, five reopened, with a hairline residual lumen in each of three.**

CONCLUSION: **This preliminary experience showed that contrast-enhanced MR angiography is a promising tool for imaging VAs; it allows the assessment of VA dissection changes over time. Most lesions tended to heal spontaneously, but persisting occlusion or pseudoaneurysm could be detected during the late course.**

Cervical artery dissections are a frequent cause of stroke in young adults (1−4). Mural hematoma usually is located within the media or the subintimal layer, leading to a ''pseudo'' enlargement of the artery (2). In most institutions, anticoagulation is used for 3 to 6 months at the acute phase to prevent thromboembolic events (3). In vertebral artery (VA) dissections, a lumbar puncture often is performed before treatment to exclude subarachnoid hemorrhage when the intradural portion of the artery is involved (5, 6).

Conventional angiography still is considered the standard of reference for the diagnosis of cervical dissection (7). The most typical aspect is a long and irregular stenosis associated with a pseudoaneurysm (4, 7, 8). Occlusive dissection is less specific because other causes of occlusion, such as thromboembolism or atherosclerotic disease, cannot be excluded by angiography (4, 9). The time course of cervical dissections remains poorly documented. A majority of patients return to normal, with improvement of luminal abnormalities (3, 4, 7). In cases of residual aneurysm, persisting severe stenosis, or underlying arteriopathy in the late course, long-term antiplatelet therapy usually is used.

Despite interest in conventional angiography, this technique carries a risk of complication (10)

Received January 4, 1999; accepted after revision April 5.

From the Departments of Neuroradiology (X.L., A.M., J.P.P.) and Neurology (C.L., O.G., D.L.), Hôpital Salengro, University Hospital of Lille, Lille, and the Medical Division (L.N.), Siemens, Saint-Denis, France.

Address reprint requests to Xavier Leclerc, MD, Service de Neuroradiologie, Hôpital Roger Salengro, Boulevard du Professeur Leclercq, 59037 Lille, France.

and does not enable assessment of the arterial wall. The evaluation of VA dissection by using noninvasive techniques remains difficult because of the small size of VAs, their deep location, frequent anatomic variations, and surrounding structures (11−15). Previous studies have shown the usefulness of 3D time-of-flight MR angiography combined with MR imaging for the diagnosis of dissection. This technique can reveal specific aspects of dissection on axial T1-weighted images; ie, a narrowed eccentric signal void (arterial lumen), a surrounding semi-lunar high signal (mural hematoma), and an increased diameter of the artery (6, 16, 17). Nevertheless, the limited imaging volume, the frequent flow-related artifacts, and the long scanning time inherent to the technique constitute the major drawbacks of this technique for imaging the vertebrobasilar system (16−18). Important advances have been made recently in MR angiography by the use of contrast material injection (19−28). The major shortening of blood related to the contrast material on T1-weighted images allows high signal intensity in vascular structures requiring large imaging volumes. Moreover, flow-related artifacts and in-plane saturation are minimized. This technique has proved valuable for imaging carotid arteries and VAs in a short scanning time (23−26). Nevertheless, accurate timing of contrast material injection and specific acquisition of *k*-space are required to optimize the contrast of the image (20, 23, 29, 30).

The purpose of the present study was to evaluate the effectiveness of a contrast-enhanced 3D MR angiographic sequence for imaging VAs in their extracranial and intradural portions and to assess the long-term course of VA dissections by using this technique.

Methods

Patients

We attempted to assess the long-term course of VA dissection by using contrast-enhanced MR angiography in 25 consecutive patients admitted between October 1993 and August 1997 to the Lille Neurology Department for suspected dissection of the VA. All patients underwent a complete etiologic workup during the acute phase, which included coagulation tests, electrocardiography, Doppler sonography of the cervical arteries, transesophageal echocardiography, and 24-hour continuous electrocardiographic monitoring. Diagnosis was based on angiographic findings in association with MR imaging and clinical features. Of the 25 patients, nine were excluded from the present study for the following reasons: uncertain dissection (n = 5), lost to follow-up (n = 2), informed consent not obtained (n = 1), and pregnancy (n = 1). The remaining 16 patients (nine men and seven women; median age, 44 years; age range, 27−54 years) were included in the present study and underwent contrast-enhanced MR angiography between September 1997 and May 1998 at a median delay of 22 months (range, 4−42 months) after the acute phase. Informed consent was obtained from all patients for contrast MR angiographic examinations. Two patients each had a dissection of both VAs, and one had a dissection of one VA and both carotid arteries. Patients received heparin at the acute phase for up to 2 weeks and then an oral administration of anticoagulant medication for 3 months. In cases of residual arterial abnormalities shown on delayed control images, long-term aspirin therapy was used.

Imaging during the Acute Phase

Conventional angiography was performed on a Integris V3000 (Philips, Best, Netherlands) in all patients within 2 weeks after onset (median, 5 days; range, 2−10 days). Arch aortograms were obtained through a femoral approach, with two oblique cervical views. When the VA seemed occluded, cervical angiography was performed after contrast material injection in the subclavian artery with the tip of the catheter close to the origin of the VA. In the other cases, test injections were made to assess the patency of proximal portions of the VAs, and then selective vertebral angiograms were obtained. Particular attention was paid to imaging the entire length of the VAs from their origins to their intradural segments. Selective angiograms of both common carotid arteries with cervical sagittal views were obtained as well. The contrast dose for the entire study did not exceed 200 mL (Omnipaque 300, Nycomed, Princeton, NJ). Angiographic findings included at least one of the following: 1) stenosis involving a long or short segment (2 cm was considered to be a short stenosis), typically irregular; 2) occlusion involving either the entire VA or only one segment of the artery; and 3) pseudoaneurysm associated with a narrowed arterial lumen. Location of dissection was defined according to the usual anatomic classification (31). The V1 to V3 segments correspond to the extracranial portion of the VA (V1 from its origin to C6, V2 from C6 to C2, and V3 from C2 to the dura), and the V4 segment corresponds to the intracranial portion of the VA from the dura to the basilar artery.

MR imaging was performed at the acute phase in 10 patients (12 dissected VAs) within 2 weeks (median, 7 days; range, 1−15 days) after clinical onset and within 1 week (median, 3 days; range, 1−6 days) after angiography. Examinations were performed on a 1.5-T superconductive unit (Magnetom Vision; Siemens Medical Systems, Erlangen, Germany) with the use of a head and neck coil. Spin-echo T1-weighted images were obtained in the axial plane from the fifth cervical vertebra to the posterior fossa, with the following parameters: 700/12/2 (TR/TE/excitations), 4-mm section thickness, 18−24-cm field of view, and 220 × 512 matrix. Fat saturation was used, and a saturation band was placed superiorly and inferiorly to the acquisition volume to suppress venous and arterial inflow signal. The diagnosis of dissection was based on a focal increase diameter of the artery with a crescentic high-signal mural hematoma surrounding a signal void.

Follow-up Contrast-Enhanced 3D MR Angiography

All examinations were performed on a 1.5-T imaging system with a 25-mT/m maximum gradient strength. A quadrature phased-array head and neck coil was used. A transverse 2D time-of-flight sequence from the aortic arch to the skull base was used before the 3D MR angiography was performed to guide the position of the 3D slab to include the entire length of both VAs. The parameters were as follows: 27/17/1; 3-mm section thickness, 50° flip angle, 25-cm field of view, and 128 × 256 matrix. Contrast 3D MR angiographic sequence was performed in the coronal plane using a fast imaging and steady-state free precession sequence, with the following parameters: 5/2, 1.5-mm section thickness, 25-cm field of view, 200 × 256 matrix, 35° flip angle, 44-second scan time. The number of sections was 40, allowing an anteroposterior coverage of 60 mm. A 100% zero-fill interpolation was performed in the section direction, and fat saturation was used. A bolus of 20 mL of gadolinium chelate (Gadodiamide Omniscan; Nycomed) was injected at a rate of 1 mL/s using an MR-compatible power injector (Spectris; Medrad, Pittsburgh, PA) and a 20-gauge intravenous catheter inserted into the antecubital vein. Injection was started at the beginning of the sequence.

Initial and follow-up imaging in 16 patients with VA dissection (involving 18 arteries)

Case (no.)	Location	Acute Phase		Follow-up			
				Angiography		MR Angiography	
		Angiography	MR Imaging	Delay (mo.)	Findings	Delay (mo.)	Findings
1	RVA: V2	Long stenosis	· · ·	3	Long stenosis	42	Occlusion
2	LVA: V2	Aneurysm	· · ·	· · ·	· · ·	23	Normal
3	LVA: V3	Long stenosis	Mural hematoma	4	Normal	26	Normal
4	RVA: V1–V4	Occlusion	Mural hematoma	4	Occlusion	21	Occlusion
5	RVA: V1–V4	Occlusion	Mural hematoma	· · ·	· · ·	4	Normal
	LVA: V4	Short stenosis	Mural hematoma				Normal
6	LVA: V3	Aneurysm	Mural hematoma	3	Irregularities	24	Normal
7	LVA: V4	Occlusion	· · ·	· · ·	· · ·	24	Aneurysm
8	LVA: V2	Short stenosis	· · ·	3	Normal	21	Normal
9	RVA: V3	Occlusion	Mural hematoma	2	Aneurysm (Contrast)	6	Normal
10	RVA: V3	Long stenosis	Mural hematoma	4	Normal	26	Normal
11	RVA: V1–V4	Occlusion	Mural hematoma	5	Normal	14	Normal
	LVA: V2	Long stenosis	Mural hematoma		Normal		Normal
12	RVA: V1–V4	Occlusion	Mural hematoma	3	Normal	8	Normal
13	LVA: V3	Long stenosis	Mural hematoma	· · ·	· · ·	7	Normal
14	LVA: V4	Occlusion	Enlargement	· · ·	· · ·	26	Occlusion
15	LVA: V3–V4	Short stenosis	· · ·	· · ·	· · ·	8	Normal
16	LVA: V3–V4	Long stenosis	· · ·	4	Normal	29	Normal

Note.—RVA, right vertebral artery; LVA, left vertebral artery.

No test bolus was performed for determining the scan delay. When no hypersignal was detected in the internal carotid artery or when the signal in the jugular vein was higher than the internal carotid artery signal, we performed a second sequence 5 to 10 minutes later using an additional 20-mL dose of gadolinium and a modified scan delay (10 seconds before the beginning of the sequence in the case of low arterial contrast and 10 seconds later in the case of major venous enhancement). The total dose ranged from 0.2 to 0.3 mmol/kg. The images then were transferred to a workstation. Subvolumes were created to isolate VAs and carotid arteries. Selective subvolumes of VAs were created as well to analyze the entire length of the arteries better. MR angiograms were generated in lateral rotations by using a maximum intensity projection algorithm and projections every 10° from −90° to +90° with 0° corresponding to the frontal plane. Follow-up using conventional angiography and MR imaging was performed as well in nine and 14 patients, respectively, at a median delay of 3 months (range, 3−5 months) and 23.5 months (range, 4−42 months).

Image Analysis

Conventional angiograms and cervical T1-weighted spin-echo MR images were reviewed by two trained radiologists (X.L., A.M.) to determine the type of dissection and the level of the involved vessels. Follow-up MR angiograms were interpreted in a consensus manner simultaneously by both radiologists, who were blinded to the results of previous examinations. Image quality was judged according to number of injections, image coverage, arterial signal, venous enhancement, and presence of artifacts. Image coverage and arterial signal were analyzed for each VA in the four arterial segments (V1, V2, V3, and V4). The absence of segment visibility of arteries was related to inadequate image coverage when the lateral views showed segment exclusion from the 3D slab. The arterial signal was judged for each arterial segment by comparing the signal between the enhanced arterial lumen and the surrounding structures. It was graded as mild when only a slight difference was detected and high when the signal within the artery appeared bright with accurate delineation of artery outlines. Venous enhancement was graded as 0 (complete isolation of the arterial phase), 1 (mild venous enhancement), or 2 (venous enhancement similar to arterial enhancement). An artery was judged nonassessable when it was excluded from the image volume and in cases of mild arterial signal or grade 2 venous enhancement. Analysis of artifacts included motion artifacts and flow-related artifacts. When the VA was judged assessable, the arterial lumen for each segment was analyzed to determine the presence of residual stenosis, pseudoaneurysm, luminal irregularities, and occlusion.

Results

Acute Phase

Clinical presentation during the acute phase mainly consisted of headache (n = 10), usually located in the occiput, and ipsilateral neck pain (n = 11). Basilar ischemic symptoms were found in 13 cases. Wallenberg's syndrome was present in two patients. Headache was isolated in two patients, and transient ischemic attack was the sole manifestation of basilar ischemia in two patients.

Of the 16 patients, 18 VAs were found to be dissected on initial angiograms obtained during the acute phase (Table 1). The most common angiographic abnormalities consisted of a short or long stenosis, often irregular and tapered (n = 11). The stenosis involved the V2 segment in four cases, the V3 in four, only the V4 in one, and both the V3 and V4 in two. In two dissected arteries, the stenosis was associated with a pseudoaneurysm (one saccular and one fusiform). A complete occlusion of the VA from V1 to V4 was found in four cases, whereas the occlusion involved only the V3 or V4 segments in three cases.

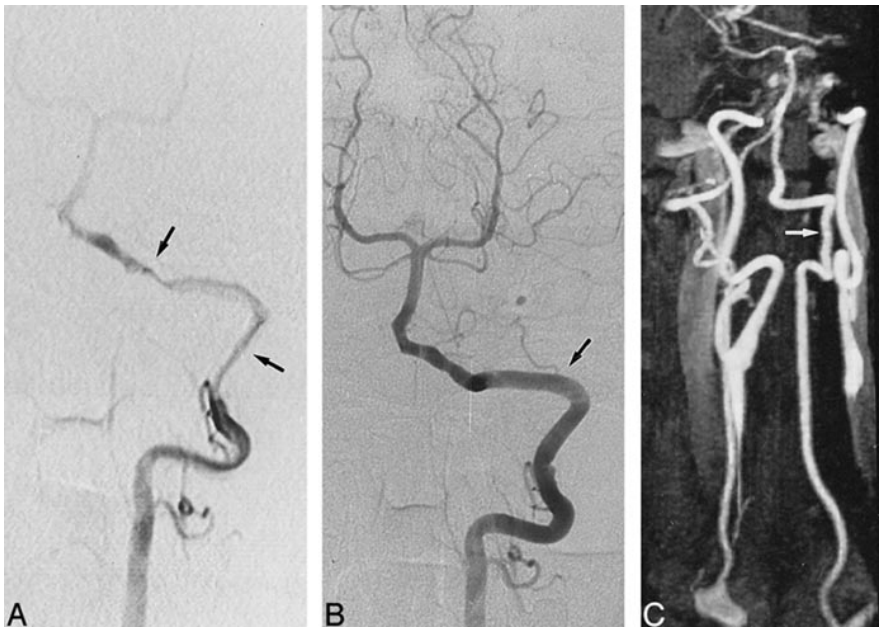

FIG 1. A 48-year-old man with occipital headaches, neck pain, and Wallenberg's syndrome.

A, Selective angiogram of the left VA shows typical aspect of stenotic dissection with a long stenosis (*arrows*) involving the V3 and V4 segments of the VA.

B, Early follow-up conventional angiogram, obtained at 4 months, shows a normal left VA (*arrow*) with complete resolution of luminal abnormalities.

C, Contrast-enhanced MR angiogram, obtained 29 months later, shows normal appearance of the left VA (*arrow*).

Of the 10 patients who underwent T1-weighted axial imaging during the acute phase, a typical aspect of dissection was found in nine patients, including a crescentic high signal (mural hematoma) surrounding a signal void (residual arterial lumen). For one patient with occlusion of the V4 segment, an enlargement of the artery was shown at the site of the dissection. In five VAs, the residual arterial lumen was not seen at initial angiography whereas T1-weighted images obtained after angiography showed a narrowed signal void related to the reopening of the artery surrounded by a mural hematoma.

Follow-up

No recurrence of stroke or transient ischemic attack was found during the period of follow-up. A complete resolution of symptoms was observed in six patients, including three with initial symptoms of basilar ischemia. Isolated residual headaches or neck pains were found in five patients. In the remaining five patients, sequelae were present, including hemianopia (n = 1), ataxia (n = 2), seventh cranial nerve palsy (n = 1), and hemiparesthesia (n = 1). No patient maintained a disabling motor deficit.

Contrast-enhanced MR angiograms showed complete isolation of the arterial phase in six patients, whereas the jugular veins were mildly enhanced in the remaining 10 patients. No grade 2 venous enhancement was observed. Nonetheless, an additional sequence with a modified timing of contrast injection was performed in two patients, related to a major enhancement of the venous structures. Image coverage was appropriate for assessing both VAs in their extracranial and intradural portions. In four small VAs, the artery was judged nonassessable in its initial portion (V1) attributable to mild contrast enhancement. Arterial signal was judged as high in the remaining cases. Motion artifacts were present in two patients but did not impact interpretation of images. In one examination, a central signal void was found throughout the arterial lumen of cervical arteries, but this did not prevent image analysis. Finally, in one patient, a carotid artery overlapped the VA and obscured the V3 segment of one VA.

The time course of the lesions showed normalization of the arterial lumen in 10 of 11 stenotic dissections (Fig 1). In one patient, a long stenosis shown to involve the V2 segment by initial MR angiography was shown to progress to occlusion by delayed MR angiography. Reopening occurred in five of seven arteries that were shown to have initial occlusion by conventional angiography (Fig 2). Of the five reopened vessels, however, the diameter of the VA was thin in each of three cases and had a hairline appearance. In two cases of occlusive dissections shown by initial angiography, the arteries remained occluded at 21 and 26 months, respectively, after the initial symptoms. The two pseudoaneurysms detected by initial conventional angiography resolved spontaneously (Fig 3). A residual pseudoaneurysm was detected by delayed MR angiography performed at 24 months, whereas the initial angiography showed a complete occlusion of the V4 segment of the VA. In one patient whose initial angiography showed an occlusion of the V3 segment of the VA, early contrast-enhanced MR angiography at 2 months showed a pseudoaneurysm whereas delayed contrast-enhanced MR angiography at 6 months showed spontaneous resolution of luminal abnormalities (Fig 4).

Early follow-up angiography performed in nine patients (10 dissected arteries) showed a complete resolution of arterial abnormalities in seven arteries and no change in two arteries. Residual irregulari-

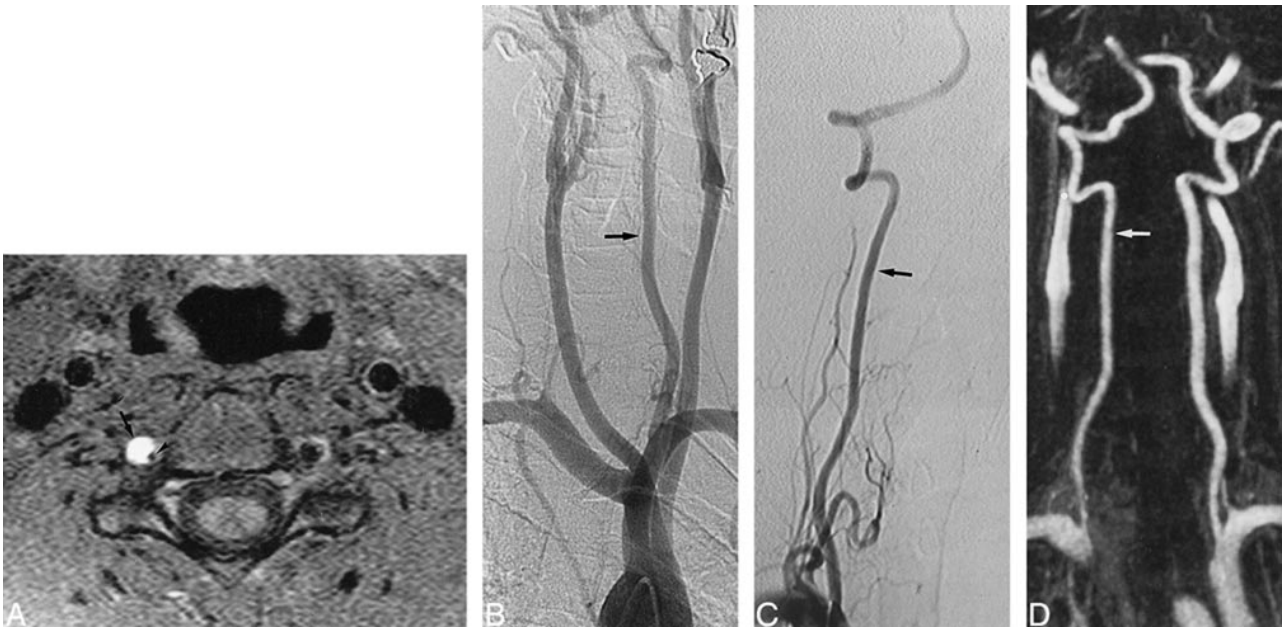

FIG 2. A 37-year-old man with neck pains and vertigo after minor cervical trauma.

A, T1-weighted axial MR image (obtained 1 day after *B*) at the C3–C4 level, shows a typical aspect of dissection of the right VA, including a crescentic high signal (*arrow*) of the mural hematoma surrounding a narrowed signal void (*arrowhead*) of the residual lumen.

B, Arch aortogram with oblique view. The left VA appears normal (*arrow*), whereas the right VA is not visible, suggesting its complete occlusion. A selective angiogram of the right subclavian artery confirmed the diagnosis of VA occlusion.

C, Oblique view selective angiogram of the right VA, obtained at 3 months, shows recanalization of the artery (*arrow*) without residual luminal irregularities.

D, Contrast-enhanced MR angiogram, obtained at 8 months, with selective subvolume MIP reconstruction of VAs, shows a normal appearance of the right VA (*arrow*), consistent with findings revealed by conventional angiography.

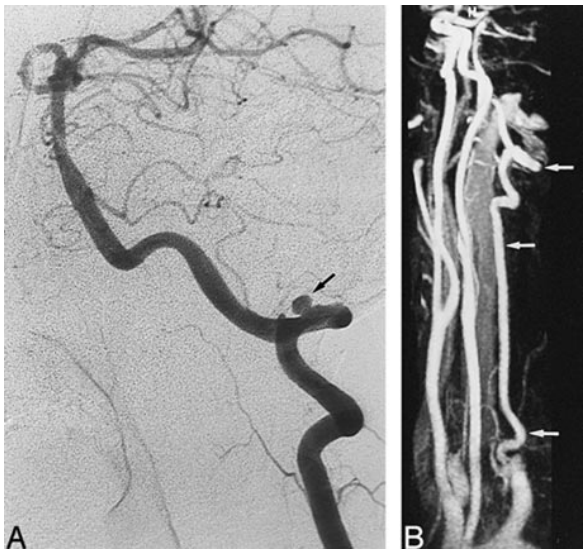

FIG 3. A 45 year-old-woman with severe headaches.

A, Oblique-view selective conventional angiogram of the left VA shows aneurysmal-type dissection, with a 3-mm-diameter pseudoaneurysm (*arrow*) involving the V3 segment of the artery.

B, Oblique view MR angiogram shows good analysis of the entire length of the left VA (*arrows*), with resolution of the pseudoaneurysm.

ties of the arterial lumen were depicted at the site of the dissection in the remaining artery, whereas the initial angiography showed a pseudoaneurysm. Follow-up MR imaging showed the disappearance of the high signal mural hematoma for all patients except one whose follow-up MR images showed a persistent high signal mural hematoma 6 months after the initial symptoms.

Discussion

Our preliminary experience showed that the entire length of the VA could be assessed by contrast-enhanced 3D MR angiography in most patients. In the case of a small VA, however, contrast enhancement of the image constituted the main limitation for analyzing the proximal portion of the artery. By using this technique, we found that most VA dissections tended to heal spontaneously. This is in agreement with angiographic studies previously reported (7, 32).

The diagnosis of VA dissection often is evoked clinically, but the clinical presentation is rarely specific. Predisposing factors and clinical symptoms reported herein were similar to those previously reported, with a history of relevant preexisting trauma in 44% of the patients and occipital neck pain in 75% (3, 4, 7). Clinical improvement has been reported to be usual in most previous reports (3, 4, 7, 9), and this is consistent with our clinical findings because resolution of symptoms was noticed in most of the patients. Minor or moderate sequelae were present in approximately one third of the patients (five patients), and none had severe residual motor deficit.

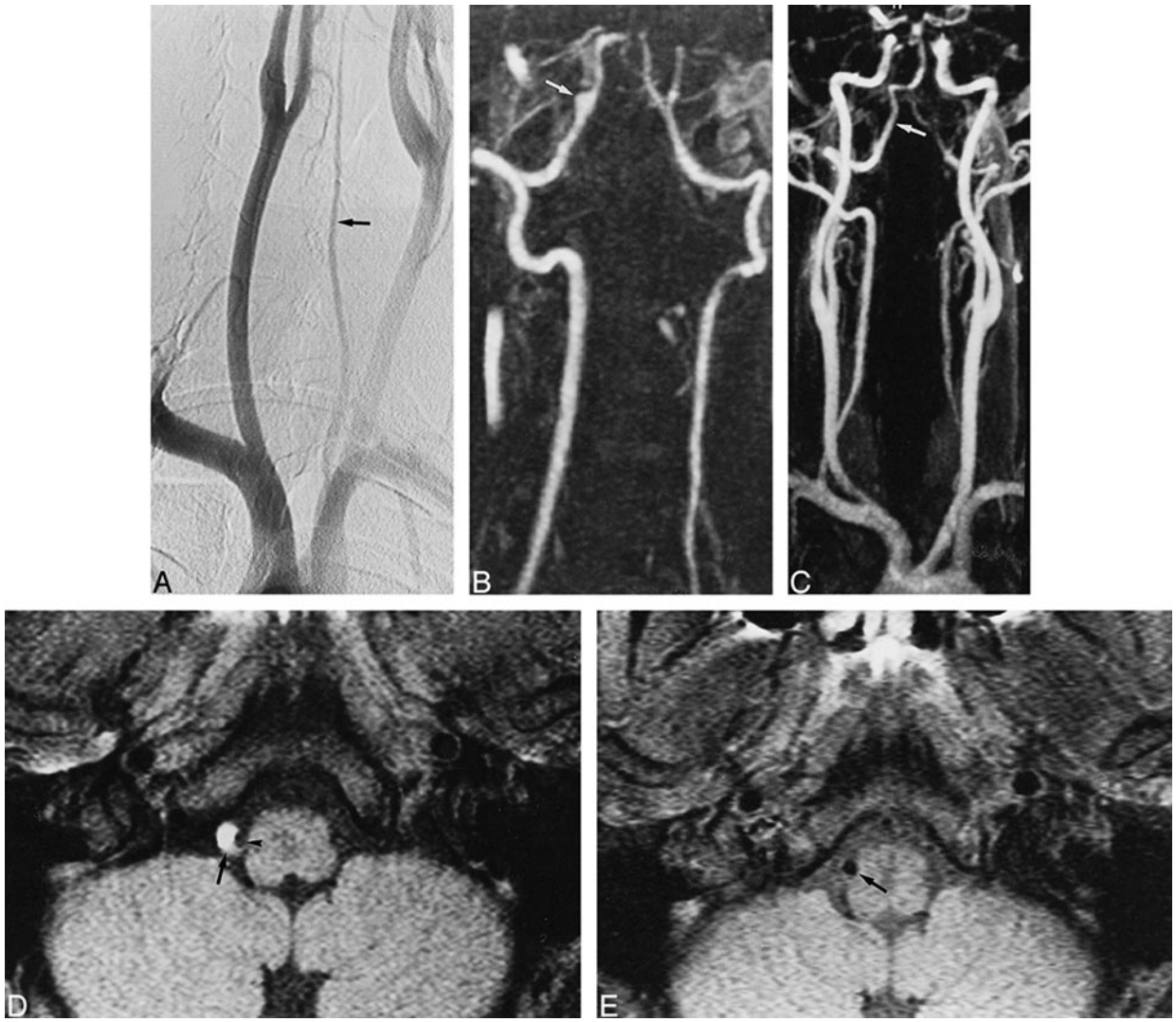

FIG 4. A 39-year-old man with neck pain and Wallenberg's syndrome.

A, Arch aortogram shows a small left VA (*arrow*), whereas the right VA is not visible.

B, Contrast-enhanced MR angiogram, obtained at 2 months, shows complete recanalization of the right VA, with a fusiform pseudoaneurysm in its intradural segment (*arrow*).

C, Contrast-enhanced MR angiogram, obtained at 6 months, shows a normal aspect of the right VA (*arrow*), with a complete resolution of the pseudoaneurysm.

D, T1-weighted MR image, obtained at 9 days, shows a typical aspect of dissection of the intradural segment of the right VA with a crescentic high signal (*arrow*) surrounding a narrowed signal void (*arrowhead*).

E, T1-weighted axial MR image, obtained at 6 months, shows a spontaneous resolution of the mural hematoma of the right VA (*arrow*).

Diagnosis of dissection at the acute phase is mainly based on angiographic findings, including elongated or tapered stenosis and pseudoaneurysm, whereas pathognomonic signs, such as double lumen or intimal flap, are rarely observed (7). In occlusive dissections, diagnosis remains uncertain because images are less specific. This explains why some authors excluded VA occlusions from their studies when conventional angiography constituted the sole technique for the diagnosis (4, 9). In this regard, MR imaging constitutes a major complementary tool for detecting cervical dissection, which appears typically on T1-weighted spin-echo images as a crescentic wall thickening with a high signal surrounding a narrowed signal void (6, 8, 16, 17). By the use of T1-weighted axial images in the present study, a typical aspect of dissection was found in five cases of occlusive dissection, even when apparent occlusion of the residual lumen was shown by conventional angiography. Despite the interest in MR imaging for the diagnosis of dissection, limitations may be emphasized. Diagnosis may be difficult during the first few days in the case of a fresh hematoma with an intermediate signal (6, 17), but this situation never has been encountered in our experience. Images remain nonspecific when the high signal covers all the section of the artery, leading to confusion between the mural hematoma and the thrombus in the true arterial lumen (33). This was observed in one patient, but the increased diameter of the artery at the level of the occluded artery allowed diagnosis of dissection.

This sign might constitute one of the best criteria for the diagnosis, as previously suggested (16, 33). Finally, VA dissections are more difficult to detect than are internal carotid artery dissections because of the length of the artery and the normal high signal of the surrounding structures, which may hinder the mural hematoma (17). Nonetheless, most VA dissections involved the distal segments of the VA and the use of a fat-suppression technique and saturation bands minimize these drawbacks.

Follow-up gadolinium-enhanced 3D MR angiography allowed accurate visualization of the entire length of both VAs in most patients. To optimize spatial resolution, our protocol included a scan time slower than that used in previous reports assessing the aorta and its major branches (19, 27, 28). We decreased the field of view and increased the matrix size to reduce the voxel size and added a zero-fill interpolation in the section direction to reduce partial-volume artifact (34). Despite these parameters, the initial segment of the VAs was not assessable in the case of a small artery and mild arterial contrast enhancement. This shortcoming will undoubtedly be overcome in the near future by using a high-resolution MR angiographic sequence. We currently are evaluating a new 3D MR angiographic acquisition technique, measuring fewer data in the *k*-space, allowing the use of thinner partitions and a 512 matrix without scanning time penalty. Arterial signal was high in the other cases, providing accurate arterial lumen analysis despite a mild venous enhancement observed in approximately half of the patients. The frequent venous enhancement observed in the present study, as compared with that of a previous report (25), may be explained by the long scanning time and the blood-brain barrier, which prevents the extraction of gadolinium from the intracerebral circulation (24). This, however, did not constitute a limiting factor for image analysis because multiple-view angles enabled separation of the arteries from the venous structures. Image contrast mainly is controlled by the center of the *k*-space, which contains low spatial frequencies, whereas the peripheral area contains high spatial frequencies and controlled spatial resolution (35). For optimal arterial contrast enhancement, it is important to time the start of injection correctly with the start of angiographic sequence so that the peak of concentration coincides with the acquisition of the mid portion of the *k*-space. By using a 44-second scanning time in the present study, the center of the *k*-space was acquired in 22 seconds, and this corresponds to the usual travel time from an antecubital vein to the cervical arteries in most patients who do not have cardiac dysfunction. Nonetheless, a second injection was required in each of two patients because of the major venous enhancement. In one case, a central signal void artifact was detected in carotid arteries. This was probably related to an acquisition of the central portion of the *k*-space before the peak of intravascular enhancement with rapid change of signal intensity along the phase-encoding direction, as previously reported (36). Methods have been reported to optimize the arterial signal. A test bolus may be performed before MR angiography (37), but this technique is time-consuming, can lead to a residual venous enhancement, and requires a power injector for better reproducibility. An MR angiographic sequence may be triggered automatically by a pulse sequence, which enables detection of the arrival of contrast material (20) or may be manually triggered by using a fluoroscopic 2D sequence combined with an elliptical centric view order (30), but these methods are not yet available. Finally, multiple time frames may be acquired during the passage of the contrast material (29), but imaging coverage remains limited and not appropriate for assessing VAs.

The time course of VA dissection on previous angiographic studies showed complete resolution of luminal abnormalities in approximately 70% of the cases (4, 7, 32). The gadolinium-enhanced 3D MR angiographic findings in our study are similar because 10 of 11 arteries that were shown to be stenosed, and four of seven arteries that were shown to be occluded by initial angiography, reverted to a normal appearance. In one patient, however, stenosis progressed to occlusion, and this seems to be uncommon in previously published cases (4, 7, 9). No residual stenosis was observed, but a hairline residual lumen of the previously occluded VA was observed in three reopened arteries. This may be related to a preexisting hypoplasia of the VA or to a change of arterial wall related to a flow drop during a long period of time, as suggested by Leclerc et al (38), who assessed the time course of internal carotid dissections by the use of CT angiography. The two pseudoaneurysms found at initial angiography in our study were shown by follow-up MR angiography to have resolved spontaneously. These results are similar to those previously reported on conventional angiography showing frequent resolution or decrement in size in most pseudoaneurysms (7, 37). In each of two cases, however, we detected a pseudoaneurysm on follow-up MR angiograms, whereas the initial angiogram showed a complete occlusion of the distal segment of the artery. To our knowledge, this unusual course has never been reported, and might be explained by the initial expansion of the mural hematoma toward the adventitia after recanalization, leading to an aneurysmal dilation of the dissected arterial segment (7). These findings suggest that gadolinium-enhanced 3D MR angiography is a suitable technique for assessing the late course of VA dissection and especially to evaluate pseudoaneurysms because of the absence of artifact. This is of particular relevance for the management of antiplatelet therapy (3, 9). Nonetheless, slight luminal abnormalities may be not detected because of the limited spatial resolution as compared with conventional angiography. MR angiography could be performed around the sixth month rather than

during the first 3 months because discrepancies may be observed between early and late control angiography. Other noninvasive methods, such as Doppler sonography or helical CT, could be interesting but seem less appropriate because of the deep location of the VA and the surrounding structures that prevent accurate analysis of vessels at the skull base (12, 13, 39).

T1-weighted axial images showed resolution of the high signal in 94% of the cases, and this suggests that most mural hematomas resolved during the first months after onset. In one patient with previously occlusive dissection, follow-up MR imaging performed at 6 months showed a persistent crescentic high signal whereas angiography showed recanalization of the artery. These findings are in agreement with those previously reported showing nonspecific signal changes of the dissecting hematoma on repeated MR images (6, 17).

Conclusion

This feasability study showed that MR angiography is a promising technique for imaging VAs; it allows the acquisition of a large volume in a short scan time without major artifact. Nevertheless, accurate analysis of the initial portion of the VA remains difficult in the case of a small artery and mild arterial contrast enhancement because of the limited spatial resolution. Moreover, contrast of image may be suboptimal when the delay between contrast material injection and data acquisition is incorrectly estimated. By the use of this technique in the present study, the time course of most VA dissections is in agreement with those of previous angiographic studies. A hairline residual lumen or a pseudoaneurysm may appear, however, during the late course of occlusive dissections. Further studies using contrast-enhanced MR angiography with a reduced voxel size are required to determine the exact role of this technique for the management of cervical artery dissections.

References

1. Bogousslavsky J, Pierre P. **Ischemic stroke in patients under age 45.** *Neurol Clin* 1992;10:113–124
2. Hart RG. **Vertebral artery dissection.** *Neurology* 1988;38:987–989
3. Leys D, Moulin T, Stojkovic T, Begey S, Chavot D, for the DONALD Investigators. **Follow-up of patients with history of cervical artery dissection.** *Cerebrovasc Dis* 1995;5:43–49
4. Mas JL, Bousser MG, Hasboun D, Laplane D. **Extracranial vertebral artery dissections. A review of 13 cases.** *Stroke* 1987;18: 1037–1047
5. Caplan LR, Baquis GD, Pessin MS, et al. **Dissection of the intracranial vertebral artery.** *Neurology* 1988;38:868–877
6. Yoshimoto Y, Wakai S. **Unruptured intracranial vertebral artery dissection. Clinical course and serial radiographic imagings.** *Stroke* 1997;28:370–374
7. Mokri B, Houser W, Sandok BA, Piepgras DG. **Spontaneous dissections of the vertebral arteries.** *Neurology* 1988;38:880–885
8. Klufas RA, Hsu L, Barnes PD, Patel MR, Schwartz RB. **Dissection of the carotid and vertebral arteries. Imaging with MR angiography.** *AJR Am J Roentgenol* 1995;164:673–677
9. Provenzale JM, Morgenlander JC, Gress D. **Spontaneous vertebral dissection. Clinical, conventionalangiographic, CTand MR findings.** *J Comput Assist Tomogr* 1996;20:185–193
10. Hessel SJ, Adams DF, Abrams HL. **Complications of angiography.** *Radiology* 1981;138:273–281
11. De Bray JM, Penisson-Besnier I, Dubas F, Emile J. **Extracranial and intracranial vertebrobasilar dissections. Diagnosis and prognosis.** *J Neurol Neurosurg Psychiatry* 1997;63:46–51
12. Hoffmann M, Sacco RL, Chan S, Mohr JP. **Noninvasive detection of vertebral artery dissection.** *Stroke* 1993;24:815–819
13. Sturzenegger M, Mattle HP, Rivoir A, Rihs F, Schmid C. **Ultrasound findings in spontaneous extracranial vertebral artery dissection.** *Stroke* 1993;24:1910–1921
14. Leclerc X, Godefroy O, Pruvo JP, Leys D. **Computed tomographic angiography for the evaluation of carotid artery stenosis.** *Stroke* 1995;26:1577–1581
15. Link J, Brossmann J, Grabener M, et al. **Spiral CT angiography and selective digital subtraction angiography of internal carotid artery stenosis.** *AJNR Am J Neuroradiol* 1996;17:89–94
16. Levy C, Laissy JP, Raveau V, et al. **Carotid and vertebral artery dissections. Three-dimensional time-of-flight MR angiography and MR imaging versus conventional angiography.** *Radiology* 1994;190:97–103
17. Mascalchi M, Bianchi MC, Mangiafico S, et al. **MRI and MR angiography of vertebral artery dissection.** *Neuroradiology* 1997;39:329–340
18. Röther JR, Wentz KU, Rautenberg W, Schwartz A, Hennerici M. **Magnetic resonance angiography in vertebrobasilar ischemia.** *Stroke* 1993;24:1310–1315
19. Bakker J, Beek FJ, Beutler JJ, et al. **Renal artery stenosis and accessory renal arteries. Accuracy of detection and visualization with gadolinium-enhanced breath-hold MR angiography.** *Radiology* 1998;207:497–504
20. Foo TKF, Saranathan M, Prince MR, Chenevert TL. **Automated detection of bolus arrival and initiation of data acquisition in fast, three-dimensional gadolinium-enhanced MR angiography.** *Radiology* 1997;203:275–280
21. Ho KY, de Haan MW, Kessels AG, Kitslaar PJ, vanEngelshoven JM. **Peripheral vascular tree stenoses. Detection with subtracted and nonsubtracted MR angiography.** *Radiology* 1998;206: 673–681
22. Ho KY, Leiner T, de Haan MW, Kessels AG, Kitslaar PJ, van-Engelshoven JM. **Peripheral vascular tree stenoses. Evaluation with moving-bed infusion-tracking MR angiography.** *Radiology* 1998;206:683–692
23. Kim JK, Farb RI, Wright GA. **Test bolus examination in the carotid artery at dynamic gadolinium-enhanced MR angiography.** *Radiology* 1998;206:283–289
24. Leclerc X, Martinat P, Godefroy O, et al. **Contrast-enhanced three-dimensional with steady-state (FISP) MR angiography of supraaortic vessels. Preliminary study.** *AJNR Am J Neuroradiol* 1998;19:1405–1413
25. Levy RA, Prince MR. **Arterial-phase three-dimensional contrast-enhanced MR angiography of the carotid arteries.** *AJR Am J Roentgenol* 1996;167:211–215
26. Remonda L, Heid O, Schroth G. **Carotid artery stenosis, occlusion, andpseudo-occlusion. First-pass, gadolinium-enhanced, three-dimensional MR angiography. Preliminary study.** *Radiology* 1998;209:95–102
27. Prince MR, Narasimham DL, Stanley JC, et al. **Breath-hold gadolinium-enhanced MR angiography of the abdominal aorta and its major branches.** *Radiology* 1995;197:785–792
28. Siegelman ES, Gilfeather M, Holland GA, et al. **Breath-hold ultrafast three-dimensional gadolinium-enhanced MR angiography of the renovascular system.** *AJR Am J Roentgenol* 1997; 168:1035–1040
29. Korosec FR, Frayne R, Grist TM, Mistretta CA. **Time-resolved contrast-enhanced 3D MR angiography.** *Magn Reson Med* 1996;36:345–351
30. Wilman AH, Riederer SJ, King BF, Debbins JP, Rossman PJ, Ehman RL. **Fluoroscopically triggered contrast-enhanced three-dimensional MR angiography with elliptical centric view order. Application to the renal arteries.** *Radiology* 1997;205:137–146
31. Francke JP, Di Marino V, Pannier M, Argenson C, Libersa C. **The vertebral arteries (arteria vertebralis).** *Anatomica Clinica* 1981; 2:229–242
32. Houser OW, Mokri B, Sundt TM, Baker HL, Reese DF. **Spontaneous cervical cephalic arterial dissection and its residuum. Angiographic spectrum.** *AJNR Am J Neuroradiol* 1984;5:27–34
33. Zuber M, Meary E, Meder JF, Mas JL. **Magnetic resonance imaging and dynamic CT scan in cervical artery dissections.** *Stroke* 1994;25:576–581

34. Du YP, Parker DL, Davis WL, Cao DG. **Reduction of partial-volume artifacts with zero-filled interpolation in three-dimensional angiography.** *J Magn Reson Imaging* 1994;4:733–741
35. Mezrich R. **A perspective on K-space.** *Radiology* 1995;195:297–315
36. Ito K, Kato J, Okada S, Kumazaki T. **K-space filter effect in three-dimensional contrast MR angiography.** *Acta Radiol* 1997; 38:173–175
37. Kim JK, Farb RI, Wright GA. **Test bolus examination in the carotid artery at dynamic gadolinium-enhanced MR angiography.** *Radiology* 1998;206:283–289
38. Leclerc X, Lucas C, Godefroy O, et al. **Helical CT for the follow-up of cervical internal carotid dissections.** *AJNR Am J Neuroradiol* 1998;19:831–837
39. Leclerc X, Godefroy O, Salhi A, Lucas C, Leys D, Pruvo JP. **Helical CT for the diagnosis of extracranial carotid artery dissection.** *Stroke* 1996;27:461–466